



Article

Fetal Radiation Dose in Common Diagnostic Radiology Procedures for Pregnant Patients: Findings from In-Phantom Measurements

Anja Tomić, Hrvoje Brkić, Tajana Turk, Mladen Kasabašić, Ivana Bjelobrk, Ivana Kralik, Francesca De Monte, Nicola Zancopè, Riccardo Lombardi, Marija Majer et al.

Special Issue









Advances and Applications of Medical Imaging Physics

Edited by
Prof. Dr. Gordana Žauhar



Article

Fetal Radiation Dose in Common Diagnostic Radiology Procedures for Pregnant Patients: Findings from In-Phantom Measurements

Anja Tomić¹, Hrvoje Brkić^{2,3} , Tajana Turk^{1,2} , Mladen Kasabašić^{1,2} , Ivana Bjelobrk¹, Ivana Kralik^{4,5} , Francesca De Monte⁶ , Nicola Zancopè⁷ , Riccardo Lombardi⁷, Marija Majer⁸, Željka Knežević⁸ , Mercedes Horvat⁸, Matko Škarica^{2,9}, Zrinka Marić², Dario Faj^{2,3,*}  and Vjekoslav Kopačin^{1,2}

¹ University Hospital Centre Osijek, 31000 Osijek, Croatia; anja.tomic93@gmail.com (A.T.); mladen.kasabasic@kbco.hr (M.K.); ika1882@gmail.com (I.B.); vkopacin@mefos.hr (V.K.)

² Faculty of Medicine, University of Josip Juraj Strossmayer, 31000 Osijek, Croatia; hbrkic@fdmz.hr (H.B.); skarica.matko@gmail.com (M.Š.); zrinka.marić@gmail.com (Z.M.)

³ Faculty of Dental Medicine and Health, University of Josip Juraj Strossmayer, 31000 Osijek, Croatia

⁴ Dubrava University Hospital, 10000 Zagreb, Croatia; ikralik@kdb.hr

⁵ School of Medicine, University of Zagreb, 10000 Zagreb, Croatia

⁶ Veneto Institute of Oncology IOV-IRCCS, 35128 Padua, Italy; francesca.demonte@iov.veneto.it

⁷ Department of Physics and Astronomy “Galileo Galilei”, University of Padova, 35121 Padua, Italy; nicola.zancopè@studenti.unipd.it (N.Z.); riccardo.lombardi.1@studenti.unipd.it (R.L.)

⁸ Ruđer Bošković Institute, 10000 Zagreb, Croatia; mmajer@irb.hr (M.M.); zknez@irb.hr (Ž.K.); mercedes.horvat@irb.hr (M.H.)

⁹ National Memorial Hospital, 32000 Vukovar, Croatia

* Correspondence: dariofaj@mefos.hr

Abstract: The diagnosis of emergent conditions during pregnancy can be delayed due to insufficient knowledge of fetal radiation doses in different imaging modalities. The aim of this article is to investigate the ranges of fetal doses in most common diagnostic and interventional radiology procedures. Procedures were carried out on an anthropomorphic phantom, Tena, representing a pregnant woman in the 18th week of pregnancy with the fetus in breech position. Different clinical scenarios using computer tomography (CT), radiography, fluoroscopy and digital subtraction angiography were selected in three teaching hospitals. Measurements were performed using radiophotoluminescent glass dosimeters placed in dedicated holes in the fetal head and fetal body. Measured fetal doses were below 1 mGy when the fetus was not in the primary beam. The highest fetal doses, up to 47 mGy, were measured after a CT scan for polytrauma and up to 24 mGy after a CT scan of the abdomen and pelvis. Significant variability in fetal doses for the same procedure was found between different hospitals but within the same hospital also. All obtained results are below the threshold for deterministic effects given by the International Commission for Radiation Protection but can be reached with two or more imaging procedures employed. The variability in fetal doses for the same procedures highlights the need for the improved optimization of imaging protocols.

Keywords: diagnostic radiology; pregnant patient; radiation dose; phantom



Academic Editor: Vladislav Toronov

Received: 12 December 2024

Revised: 20 January 2025

Accepted: 22 January 2025

Published: 23 January 2025

Citation: Tomić, A.; Brkić, H.; Turk, T.; Kasabašić, M.; Bjelobrk, I.; Kralik, I.; De Monte, F.; Zancopè, N.; Lombardi, R.; Majer, M.; et al. Fetal Radiation Dose in Common Diagnostic Radiology Procedures for Pregnant Patients: Findings from In-Phantom Measurements. *Appl. Sci.* **2025**, *15*, 1143. <https://doi.org/10.3390/app15031143>

Copyright: © 2025 by the authors.

Licensee MDPI, Basel, Switzerland.

This article is an open access article distributed under the terms and

conditions of the Creative Commons Attribution (CC BY) license

(<https://creativecommons.org/licenses/by/4.0/>).

1. Introduction

Emergent, potentially life-threatening conditions during pregnancy can also be of non-obstetric etiology. Due to the physiological and anatomical changes that occur during pregnancy, the female body becomes five times more susceptible to thrombotic incidents,

with venous thromboembolism being the leading cause of maternal death in developed countries [1–3]. Pregnancy-associated stroke is known to cause 18% of strokes in women under the age of 35, causing up to 15% of the deaths of pregnant women worldwide [4–6]. Other potentially life-threatening conditions can be singled out, such as appendicitis, being the most common non-obstetric complication in pregnancy that requires surgical intervention with a reported frequency of 1 in 500–2000 pregnancies [7]. The second most common cause of acute abdomen that requires surgical treatment in pregnant women is cholecystitis, with the incidence being the same as that in the general population [8,9]. Nephrolithiasis is also one of the causes of abdominal pain in pregnancy, with the reported incidence varying from 1 in 250 to 300 [10]. Furthermore, 1 in 12 pregnant women experience trauma during pregnancy, which often requires the use of extensive diagnostics [11].

Although current guidelines state that diagnostic imaging procedures using ionizing radiation should not be avoided in pregnant patients if there is a good risk–benefit ratio, the diagnosis of such conditions can often be delayed due to the fear of using ionizing radiation during pregnancy and the unavailability of other diagnostic modalities such as magnetic resonance imaging [12,13]. A lack of knowledge coupled with patients' fears can result in the avoidance of procedures or even unnecessary pregnancy terminations, underscoring the importance of knowledge of fetal doses in different clinical scenarios, as well as optimization of the procedures [14,15]. This fear is present due to a known deterministic effect on fetuses which occurs with doses above 100 mGy and includes growth restriction, cognitive impairment, congenital malformations, etc. [16]. Besides deterministic effects, stochastic effects may occur. For stochastic effects, no dose threshold exists, but the risk increases with radiation dose. It has been reported that with higher fetal doses such as doses delivered during a CT scan of the pelvis, the risk of carcinogenesis increases, but it is still low in absolute terms, approximately 1 in 250 [17].

It is considered unethical to conduct dosimetry experiments involving ionizing radiation on pregnant patients due to the potential risks to the fetus. Instead, researchers often rely on phantom measurements, computational models, or some other fetal dose estimation methods, reporting a wide range of values for different scanning protocols [18–22].

The aim of this study was to investigate the range of fetal doses in the most common clinical scenarios using diagnostic and interventional radiology procedures during pregnancy in three large teaching hospitals. The obtained data will contribute to the general knowledge of fetal doses in different clinical scenarios and reasons for their variations. This will help in raising awareness about the need for the optimization of radiological procedures and can help to avoid unnecessary delays in providing the necessary diagnostic procedures in pregnancy in some cases.

2. Materials and Methods

The imaging procedures were carried out on an anthropomorphic phantom, Tena, representing a pregnant woman in the 18th week of pregnancy with the fetus in breech position in the uterus [23,24]. The phantom includes the head and neck, thorax, abdomen, and pelvis to the proximal thighs. It is 88.9 cm high, without holding brackets, and divided into 18.5 cm thick slices. It consists of three types of substitute tissues, soft tissue substitution (STS), bone tissue substitution (BTS), and lung tissue substitution (LTS), as seen in Figure 1, with the physical and radiological properties listed in Table 1.

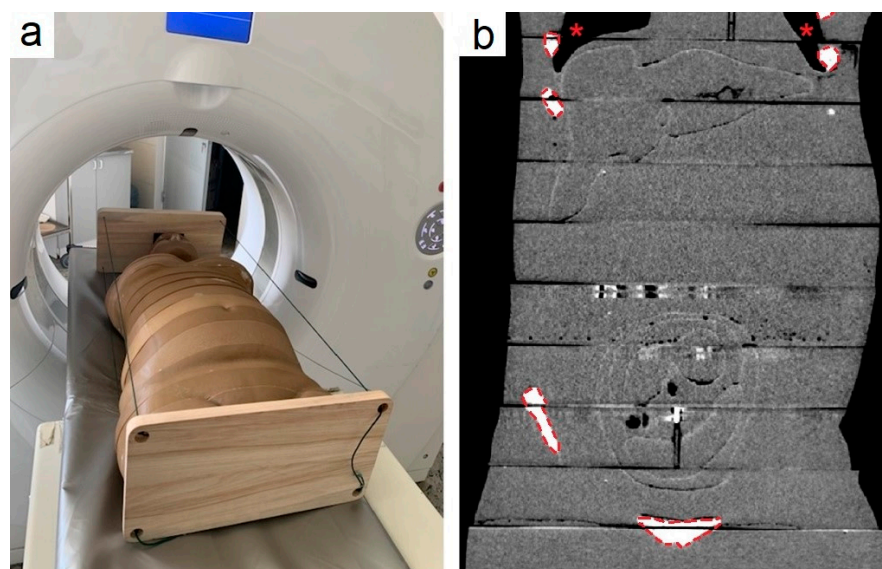


Figure 1. Anthropomorphic physical phantom, Tena, placed inside the CT scanner gantry (a). A coronal plane of the CT scan of the phantom (b) showing its composition, BTS (dashed red lines), LTS (red asterisk), and STS (rest).

Table 1. Physical and radiological properties of substitution tissues used in the Tena physical phantom. PU—polyurethane, HU—Hounsfield units, Z_{eff} —effective atomic number.

| Anatomical Region | Head, Neck, Thorax, Abdomen, Pelvis, Proximal Parts of the Thighs |
|---|---|
| Height (cm)/Mass (kg) | 88.9/49.7 |
| Substitutional Tissues | |
| STS | PU rubber, CaCO_3 |
| Mass density (g/cm^3) | 1.03 |
| CT number (HU) | 30 ± 5 |
| Z_{eff} | 6.94 |
| BTS | Epoxy resin, CaCO_3 , SiO_2 |
| Mass density (g/cm^3) | 1.274 |
| CT number (HU) | 450 ± 45 |
| Z_{eff} | 10.78 |
| LTS | STS, polystyrene (Styrofoam) balls |
| Mass density (g/cm^3) | 0.29 |
| CT number (HU) | -750 ± 80 |
| Z_{eff} | 6.9 |

Research was conducted in two large teaching hospitals in Croatia and one in Italy (herein randomly named Hospital 1, Hospital 2, and Hospital 3). Considering the occurrence of non-obstetric emergencies in pregnancy, five clinical scenarios were selected for the research in the first stage in Hospital 1—nephrolithiasis/ileus/abdominal pain, nephrostomy placement due to nephrolithiasis/urolithiasis, polytrauma, pulmonary embolism, and ischemic stroke. Conventional radiography, CT, fluoroscopy, and fluoroscopy/digital subtraction angiography were chosen as imaging modalities.

For the clinical scenario of non-specific abdominal pain, two protocols were simulated—abdomen and pelvis radiography in two positions and non-contrast CT (NCCT) of the abdomen and pelvis, with a scanning volume from the lung bases to the greater trochanters. Pulsed fluoroscopy was simulated in a clinical scenario of nephrostomy tube placement. In a clinical scenario of polytrauma, an institutional protocol was used consisting of a

non-contrast CT of the head and cervical spine, thorax and abdomen (simulating arterial phase), and abdomen and pelvis (simulating venous phase). CT angiography (CTA) of the pulmonary arteries with bolus tracking ($5\times$) was simulated in a clinical scenario of pulmonary embolism. For the clinical scenario of ischemic stroke, a stroke protocol for diagnosis was simulated consisting of an NCCT of the head and CTA of the aortic arch up to the vertex. In the therapeutic part, a mechanical thrombectomy for stroke was simulated, consisting of pulsed fluoroscopy for selective catheterization and mechanical thrombectomy with two passes of aspiration catheter and a DSA for pre- and post-procedural angiography. This simulation was based on a real-life stroke case in a female of a similar age to the physical phantom patient's age.

Selected clinical scenarios, imaging modalities, used devices, scanning protocols, and imaging parameters used in Hospital 1 are summarized in Table 2.

Table 2. Clinical scenarios performed in Hospital 1, imaging modalities, scanning protocols, and imaging parameters used in Hospital 1. N/A—not available, CT—computed tomography, NCCT—non-contrast CT, CECT—contrast-enhanced CT, CTA—CT angiography, PA—pulmonary artery, MT—mechanical thrombectomy, DSA—digital subtraction angiography.

| Clinical Scenario | Imaging Modality | Unit | Imaging Protocol | Imaging Parameters |
|---|---------------------|---------------------------|--|--|
| Non-specific abdominal pain | Radiography | Siemens Luminos dRF Max | Abdomen and pelvis in two positions | 80.8 kV; 18.85 mAs 72.9 kV; 40.7 mAs |
| Nephrostomy tube placement Nephro/urolithiasis | Fluoroscopy | Siemens Uroscop Omnia Max | Pulsed fluoroscopy, collimated field | N/A |
| Nephrolithiasis, appendicitis, abdominal pain | CT | GE Revolution Frontier | NCCT abdomen and pelvis (lung bases—great trochanters) | 120 kV; auto mAs (range 50–750); noise index 13.3; section thickness 5 mm; pitch 1.375:1 |
| Polytrauma | CT | GE Revolution Frontier | NCCT head | 120 kV; auto mAs (range 100–335); noise index 3.23; section thickness 2.5 mm; pitch 0.531:1 |
| | | | NCCT C spine | 120 kV; 335 mAs; section thickness 0.625 mm; pitch 0.516:1 |
| | | | CECT (35 s) thorax and abdomen | 120 kV; auto mAs (range 100–600), noise index 18; section thickness 5 mm; pitch 1.375:1 |
| | | | CECT (75 s) abdomen and pelvis | 120 kV; auto mAs (range 100–600), noise index 18; section thickness 5 mm; pitch 1.375:1 |
| Pulmonary embolism | CT | GE Revolution Frontier | CT angiography of PA with “bolus tracking” ($5\times$) | 120 kV; auto mAs (range 150–800); noise index 28; section thickness 0.625 mm; pitch 1.375:1 |
| Ischemic stroke | CT | GE Revolution Frontier | NCCT head | 120/140 kV; 400/600 mAs; |
| | | | CTA aortic arch–vertex | 120 kV; auto mAs (range 80–700), noise index 8.94; section thickness 1.25 mm; pitch 0.984:1 |
| | Fluoroscopy and DSA | Philips Azurion | 2 pass MT: Pulsed fluoroscopy for selective catheterization and MT DSA run for pre- and post-procedure angiography (6 fps) | 75 kV; 7–22 mAs Rotation 0°, LAO 45°, LAO 89° Angulation: 0° and CRAN 15° SID: 100–111 cm |

Significant fetal doses were expected only in clinical scenarios with the fetus in the primary beam [14,18–22], and these scenarios were further investigated in all three hospitals. Fetal doses were measured for conventional radiography of the abdomen, CT of the abdomen, and CT for polytrauma in an additional 3 radiography and 7 CT units in all hospitals using their own protocols. Selected clinical scenarios, imaging modalities,

equipment used, scanning protocols, and imaging parameters are summarized in Table 3 for all three hospitals.

Table 3. Clinical scenarios, imaging modalities, scanning protocols, and imaging parameters used in dosimetry measurements. CT—computed tomography, NCCT—non-contrast CT, CECT—contrast-enhanced CT. Radiography and CT units are labeled to facilitate its use further in the figures.

| Clinical Scenario | Imaging Modality | Hospital | Unit | Imaging Protocol | Imaging Parameters |
|---|------------------|----------|-------------------------------|--|---|
| Non-specific abdominal pain | Radiography | 1 | Siemens Luminos (R1) | Abdomen and pelvis in two positions | 80.8 kV; 18.85 mAs 72.9 kV; 40.7 mAs |
| | | 1 | Siemens Ysio Max (R2) | Abdomen and pelvis in AP projection | 72.9 kV; 34.99 mAs |
| | | 2 | Siemens Luminos (R1) | Abdomen and pelvis in AP projection | 72.9 kV; 62.44 mAs |
| | | 3 | Siemens Aristos (R1) | Abdomen and pelvis in two positions | 81 kV; 22 mAs 81 kV; 76 mAs |
| Nephrolithiasis, appendicitis, abdominal pain | CT | 1 | GE Revolution Frontier (CT1) | NCCT abdomen and pelvis (lung bases—great trochanters) | 120 kV; CTDI 17.0 mGy; DLP 846 mGycm |
| | | 1 | Siemens Definition As (CT2) | NCCT abdomen and pelvis (lung bases—great trochanters) | 120 kV; CTDI 7.1 mGy; DLP 334 mGycm |
| | | 1 | Philips Ingenuity (CT3) | NCCT abdomen and pelvis (lung bases—great trochanters) | 140 kV; CTDI 14.3 mGy; DLP 744 mGycm |
| | | 1 | Siemens X.cite (CT4) | NCCT abdomen and pelvis (lung bases—great trochanters) | 120 kV; CTDI 10.2 mGy; DLP 513 mGycm |
| | | 2 | Siemens X.cite (CT1) | NCCT abdomen and pelvis (lung bases—great trochanters) | 120 kV; CTDI 10.8 mGy; DLP 585 mGycm |
| | | 2 | Siemens Definition As (CT2) | NCCT abdomen and pelvis (lung bases—great trochanters) | 80 kV; CTDI 1.7 mGy; DLP 100 mGycm |
| | | 3 | GE Revolution EVO (CT1) | NCCT abdomen and pelvis (lung bases—great trochanters) | 120 kV; CTDI 14.5 mGy; DLP 810 mGycm |
| | | 3 | Siemens Definition Edge (CT2) | NCCT abdomen and pelvis (lung bases—great trochanters) | 120 kV; CTDI 10.1 mGy; DLP 566 mGycm |
| Polytrauma | CT | 1 | GE Revolution Frontier (CT1) | NCCT head | 120 kV; CTDI 62.9 mGy; DLP 1035 mGycm |
| | | | | NCCT C spine | 120 kV; CTDI 36.4; DLP 735 mGycm |
| | | | | Art CECT thorax and abdomen | 120 kV; CTDI 8.0 mGy; DLP 435 mGycm |
| | | | | Venous CECT abdomen and pelvis | 120 kV; CTDI 12.4 mGy; DLP 628 mGycm |
| | | 1 | Philips Ingenuity (CT3) | NCCT head and neck | 120 kV; CTDI 49.0 mGy; DLP 1064 mGycm |
| | | | | Venous CECT thorax and abdomen and pelvis | 120 kV; CTDI 12.0 mGy; DLP 878 mGycm |
| | | 1 | Siemens X.cite (CT4) | NCCT head | 120 kV; CTDI 73.0 mGy; DLP 1142 mGycm |
| | | | | NCCT C spine | 90 kV; CTDI 19.3 mGy; DLP 354 mGycm |
| | | | | Venous CECT thorax and abdomen and pelvis | 120 kV; CTDI 10.8 mGy; DLP 747 mGycm |
| | | 2 | Siemens X.cite (CT1) | NCCT head | 120 kV; CTDI 56.4 mGy; DLP 1335 mGycm |
| | | | | NCCT C spine | 120 kV; CTDI 16.8 mGy; DLP 359 mGycm |
| | | | | NCCT thorax and abdomen and pelvis | 120 kV; CTDI 9.5 mGy; DLP 669 mGycm |
| | | | | Venous CECT thorax and abdomen and pelvis | 100 kV; CTDI 7.8 mGy; DLP 535 mGycm |
| | | 2 | Siemens Definition As (CT2) | NCCT head | 120 kV; CTDI 68.5 mGy; DLP 1450 mGycm |
| | | | | NCCT C spine | 120 kV; CTDI 11.5 mGy; DLP 224 mGycm |
| | | | | NCCT thorax and abdomen and pelvis | 120 kV; CTDI 8.4 mGy; DLP 571 mGycm |
| | | | | Venous CECT thorax and abdomen and pelvis | 100 kV; CTDI 8.4 mGy; DLP 575 mGycm |
| | | 3 | GE Revolution EVO (CT1) | NCCT head and neck | 120 kV; CTDI 55.0 mGy; DLP 980 mGycm |
| | | | | NCCT thorax and abdomen and pelvis | 100 kV; CTDI 10.5 mGy; DLP 880 mGycm |
| | | | | Art CECT thorax and abdomen and pelvis | 100 kV; CTDI 10.5 mGy; DLP 880 mGycm |
| | | | | Venous CECT thorax and abdomen and pelvis | 100 kV; CTDI 10.5 mGy; DLP 880 mGycm |
| | | 3 | Siemens Definition Edge (CT2) | NCCT head and neck | 120 kV; CTDI 77.0 mGy; DLP 1960 mGycm |
| | | | | NCCT thorax and abdomen and pelvis | 120 kV; CTDI 10.0 mGy; DLP 730 mGycm |
| | | | | Art CECT thorax and abdomen and pelvis | 120 kV; CTDI 10.0 mGy; DLP 560 mGycm |
| | | | | Venous CECT thorax and abdomen and pelvis | 120 kV; CTDI 10.0 mGy; DLP 560 mGycm |

Tena phantom is designed to have 51 possible dosimetry positions in total. For this specific research, dosimeters were positioned only in place of the fetal head and fetal body. Measurements were made using radiophotoluminescent (RPL) dosimeters (ATGC, Tokyo, Japan) which are silver-activated phosphate glass rods encapsulated in plastic holders. In recent years, RPL glass dosimeters have been recognized and more widely used as they possess good characteristics such as low fading effects, excellent dose linearity, no need for individual sensitivity correction factor, and they are easy to handle. In our previous study, the energy dependence of the GD-352M RPL dosimeter system in air was found to be better than that of the TLD systems for N-series quality beam [25]. One of their main advantages over the conventionally used TLD is the possibility for multiple readout repeatability which enhances measurement accuracy. In this study, GD-352M types were used, consisting of a glass rod (Φ 1.5 mm \times 12 mm) packed in a plastic holder (Φ 4.3 \times 14.5 mm). A plastic holder contains an energy compensation filter necessary for dosimetry in medium- and low-energy photon fields usually used in diagnostic radiology. The RPL measurements were performed with a Dose Ace FGD-1000 reader (ATGC, Tokyo, Japan) [26]. The calibration of dosimeters was performed in the ^{137}Cs gamma field in the “Secondary Standard Dosimetry Laboratory” (SSDL) of the Ruđer Bošković Institute, Zagreb, Croatia [27]. Results are expressed as absorbed dose to water. For the dose range in this study, the uncertainty of RPL dosimeters is $\sim 2.1\%$ [25]. More information about the characterization and measuring cycle of RPL dosimeters can be found in Knežević et al., 2011 and 2013 [25,28]. Due to time limitations when performing measurements in hospitals, only three measurements per protocol and per unit for all clinical scenarios and hospitals were performed in order to have as many protocols and units included. The results were presented as a mean of three measurements. The uncertainty in the estimate of the mean was quantified and presented by standard error of the mean (SEM).

3. Results

Fetal doses measured in each clinical scenario in Hospital 1 are listed in Table 4.

Table 4. Absorbed dose for each specific clinical scenario measured in the fetal head and body. CT—computed tomography, DSA—digital subtraction angiography.

| Clinical Scenario | Imaging Modality | Unit | Fetal Dose—Head (mGy) | Fetal Dose—Body (mGy) |
|---|---------------------|---------------------------|-----------------------|-----------------------|
| Non-specific abdominal pain | Radiography | Siemens Luminos dRF Max | 1.6 | 1.9 |
| Nephrostomy tube placement nephro/urolithiasis | Fluoroscopy | Siemens Uroscop Omnia Max | 0.5 | 0.1 |
| Nephrolithiasis, appendicitis, abdominal pain | CT | GE Revolution Frontier | 23.7 | 19.6 |
| Polytrauma | CT | GE Revolution Frontier | 34.7 | 32.5 |
| Pulmonary embolism | CT | GE Revolution Frontier | 0.3 | 0.2 |
| Ischemic stroke | CT | GE Revolution Frontier | 0.05 | 0.03 |
| | Fluoroscopy and DSA | Philips Azurion | 0.0 | 0.02 |

Since, as expected, measured fetal doses were always below 1 mGy if the fetus was not in the primary beam, only clinical scenarios with a fetus in the primary beam were additionally investigated. Fetal doses in all clinical scenarios with the fetus positioned in the primary beam are presented in Figure 2 for all three hospitals.

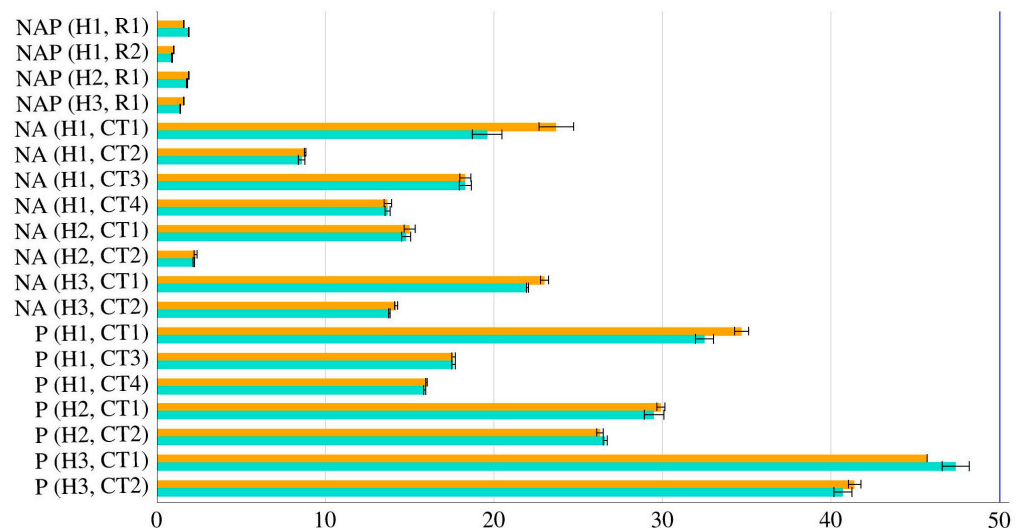


Figure 2. Absorbed dose for each specific scenario measured in the fetal head and body in three hospitals. NAP—non-specific abdominal pain; NA—nephrolithiasis, appendicitis, abdominal pain; P—polytrauma; R—radiography unit as labeled in Table 3; CT—computed tomography unit as labeled in Table 3; H—hospital. The line represents a fetal dose of 50 mGy, which the American College of Radiology suggests as an upper threshold for pelvic CT imaging protocols for a pregnant patient [29]. Uncertainty of the mean is presented with SEM.

The highest measured absorbed dose in the fetus was measured in a polytrauma CT scan scenario (consisting of head, cervical spine, thorax/abdomen, and pelvis CT) resulting in absorbed doses to the fetal head and to the fetal body of 45.7 mGy and 47.4 mGy, respectively.

4. Discussion

The simulation of the most frequent clinical scenarios involving pregnant patients and ionizing radiation diagnostic and interventional procedures (Table 2) showed a large range of possible fetal doses (Table 4) in these procedures. Nevertheless, in scenarios when the fetus is not in the primary beam, such as CTPA, CT for ischemic stroke, nephrostomy placement, or two-pass mechanical thrombectomy, the fetal head and body doses were well below 1 mGy (Table 4). This is in line with already reported values [18–22,30–32]. Such radiation doses further reinforce the fact that these procedures should not be postponed if the only contraindication is fear of fetal radiation.

Since fetal dose estimation is usually not necessary unless the dose to the fetus is expected to be above 1 mGy [14,15,20], further investigation of fetal doses was focused on clinical scenarios with a fetus within the beam. **These scenarios included abdominal radiography and CT for polytrauma in three large teaching hospitals using four radiography units and eight CT units (Table 3).**

Measured fetal doses ranged from 0.9 mGy to 1.9 mGy in abdominal radiography (Figure 2). This is in line with previous findings where fetal doses of up to 3 mGy were reported [17]. **Although fetal doses in abdominal radiography were rather consistent in all three hospitals, it is worth noting that different imaging protocols were used. Protocols consisted of one or two patient positions.** This difference was found between hospitals, but also in Hospital 1 (Table 3). Although still in use, abdominal radiography is of limited diagnostic value in a patient presenting with abdominal pain. According to the guidelines, anteroposterior projection with a patient in the supine position is a preferred method, used in a clinical scenario of suspected bowel obstruction and urinary tract calculosis [33]. If there is a clinical suspicion of possible bowel perforation, additional anteroposterior projection

with a patient in an erect position adds valuable clinical information; therefore, in several instances in this study, both patient positions were used. **This underlines importance of a clear clinical question in referral.** Nevertheless, the largest fetal dose was found in Hospital 2, which used imaging in only one patient position. This shows that attention toward the optimization of imaging procedures is required.

When a clinical question for abdominal pain was set, NCCT was a preferred scanning protocol since it also allows for the detection of urinary tract calculi, which might not always be detected on post-contrast scans. After the evaluation of NCCT scans, the radiologist might add an additional scan in the post-contrast arterial or portovenous phase. Although the standardization of all protocols is of utmost importance, it is particularly challenging in a pregnant patient, where the presentation of various clinical scenarios can differ from a non-pregnant patient. Therefore, individualized scanning protocols based on relevant clinical information are often used. In Hospital 2, a specific low-dose protocol for kidney stones was used with the low fetal dose of 2.2 mGy in one CT unit. All abdomen protocols used were routine abdomen protocols with fetal doses ranging from 8.6 mGy to 23.7 mGy (Figure 2). **This reveals a fetal dose max/min ratio of approximately three if the procedure is performed in a different hospital or even in the same hospital, but on a different unit.**

Similar findings to those in CT for abdominal pain were found in CT for polytrauma (Figure 2). The dose ranged from 15.9 mGy to 47.4 mGy when all hospitals and all eight CT units were taken into account. **These differences are mainly due to different protocols with different numbers of phases used** (Table 3). This was expected since a whole-body tomography scan is performed in various protocols and there is no agreement as to which protocol is optimal in an emergency situation [34,35]. An unenhanced scan is sometimes built into the protocol [36,37], but the Royal College of Radiologists [38] is of the opinion that an unenhanced scan of the body is of no benefit to polytrauma patients. Nevertheless, a narrower range of fetal doses was found in polytrauma than in abdominal CT within the same hospitals. This is due to the similar CT protocols used within one hospital for polytrauma, **while for abdominal CT, protocols differed in doses per phase, but also in the number of phases** (Table 3). This again shows the need for the optimization and harmonization of radiological practice.

The results presented in this study are always below 100 mGy, which is the threshold for deterministic effects indicated by the International Commission for Radiation Protection [14]. Nevertheless, in the case of repeated CT procedures of the abdomen or additional phases used, fetal doses could reach higher values that could lead to possible deterministic radiation effects on the fetus. Since different clinical scenarios justify the use of the aforementioned diagnostic procedures, especially in the case of scarce diagnostic information gained from ultrasound examination and/or the inadequacy of magnetic resonance imaging [12,13], it is important to use well-optimized imaging protocols. This underlines another finding of this study: **large variability in fetal doses for the same procedures between different hospitals, but also within the same hospital. Besides large fetal dose differences, this can also imply significant differences in diagnostic information obtained.** Although the fetal risk of developing malignant disease in childhood is small, it can be changed using different protocols, which raises the importance of the implementation of strategies for reducing radiation exposure, without compromising the quality of diagnostic data obtained [19].

Through using the freely available, inexpensive physical phantom, Tena, developed by our group [23,24], fetal dosimetry data in diagnostic imaging procedures were further improved. Additionally, the fetal dose dependance of imaging protocols was confirmed. Nevertheless, exposure of the fetus also depends on the gestational age, maternal body habitus, and fetal depth. In addition, a fetus in the second trimester can freely move within

the placenta, and there is a possibility that the radiation dose for fetuses in the cephalic position could differ for different positions. For this reason, further studies of fetal dose for differently constructed phantoms and acquisition parameters are needed.

Patient doses in diagnostic and interventional radiology procedures are optimized, and in most imaging modalities, reduced nowadays. This calls for repeated measurements of patient doses. The results presented in this work could help to better understand the radiation safety of pregnant patients and improve radiation protection measures and the optimization of imaging procedures for pregnant patients. The obtained data contribute to the general knowledge of fetal doses during diagnostic and interventional radiology procedures and to the prevention of unnecessary delays in providing the necessary procedures in pregnancy. Additionally, the presented variability in fetal doses for the same procedures highlights the need for the improved optimization of imaging protocols.

Author Contributions: Conceptualization, D.F., A.T. and V.K.; methodology, H.B., I.K., M.K., Ž.K., M.M., M.H. and T.T.; validation, I.B. and M.Š.; formal analysis, D.F. and Z.M.; investigation I.B., I.K., F.D.M., N.Z. and R.L.; data curation, All; writing—original draft preparation, A.T., V.K. and D.F.; writing—review and editing, all; supervision, D.F.; project administration, H.B.; funding acquisition, D.F. and H.B. All authors have read and agreed to the published version of the manuscript.

Funding: This research was funded by EU-funded project SONORA—Towards safe, optimized, and personalized radiology and radiotherapy procedures for pregnant patients, grant number (PI-ANOFORTE HORIZON-EURATOM-2021-NRT-01-09) and institutional projects IP—MEFOS and IP FDMZ.

Institutional Review Board Statement: Not applicable.

Informed Consent Statement: Not applicable.

Data Availability Statement: The original contributions presented in the study are included in the article, further inquiries can be directed to the corresponding author.

Conflicts of Interest: The authors declare no conflicts of interest. The funders had no role in the design of the study; in the collection, analyses, or interpretation of data; in the writing of the manuscript; or in the decision to publish the results.

References

1. Devis, P.; Knuttinen, M.G. Deep venous thrombosis in pregnancy: Incidence, pathogenesis and endovascular management. *Cardiovasc. Diagn. Ther.* **2017**, *7* (Suppl. 3), S309–S319. [\[CrossRef\]](#)
2. Say, L.; Chou, D.; Gemmill, A.; Tunçalp, Ö.; Moller, A.B.; Daniels, J.; Gülmezoglu, A.M.; Temmerman, M.; Alkema, L. Global causes of maternal death: A WHO systematic analysis. *Lancet Glob. Health* **2014**, *2*, e323–e333. [\[CrossRef\]](#) [\[PubMed\]](#)
3. Van Der Pol, L.M.; Tromeur, C.; Bistervels, I.M.; Ni Ainle, F.; Van Bommel, T.; Bertolotti, L.; Couturaud, F.; van Dooren, Y.P.; Elias, A.; Faber, L.M.; et al. Pregnancy-Adapted YEARS Algorithm for Diagnosis of Suspected Pulmonary Embolism. *N. Engl. J. Med.* **2019**, *380*, 1139–1149. [\[CrossRef\]](#)
4. Foo, L.; Bewley, S.; Rudd, A. Maternal death from stroke: A thirty year national retrospective review. *Eur. J. Obstet. Gynecol. Reprod. Biol.* **2013**, *171*, 266–270. [\[CrossRef\]](#) [\[PubMed\]](#)
5. Ijäs, P. Trends in the Incidence and Risk Factors of Pregnancy-Associated Stroke. *Front. Neurol.* **2022**, *13*, 833215. [\[CrossRef\]](#) [\[PubMed\]](#)
6. Miller, E.C.; Gatollari, H.J.; Too, G.; Boehme, A.K.; Leffert, L.; Elkind, M.S.; Willey, J.Z. Risk of Pregnancy-Associated Stroke Across Age Groups in New York State. *JAMA Neurol.* **2016**, *73*, 1461–1467. [\[CrossRef\]](#)
7. Mangal, R.; Stead, T.G.; Ganti, L.; Rosario, J. Diagnosing Appendicitis in Pregnancy Via Ultrasonography. *Cureus* **2019**, *11*, e5562. [\[CrossRef\]](#)
8. Zachariah, S.K.; Fenn, M.; Jacob, K.; Arthungal, S.A.; Zachariah, S.A. Management of acute abdomen in pregnancy: Current perspectives. *Int. J. Womens Health* **2019**, *11*, 119–134. [\[CrossRef\]](#)
9. Dietrich, C.S., III; Hill, C.C.; Hueman, M. Surgical diseases presenting in pregnancy. *Surg. Clin. N. Am.* **2008**, *88*, 403–419. [\[CrossRef\]](#)

10. Lee, M.S.; Fenstermaker, M.A.; Naoum, E.E.; Chong, S.; Van de Ven, C.J.; Bauer, M.E.; Kountanis, J.A.; Ellis, J.H.; Shields, J.; Ambani, S.; et al. Management of Nephrolithiasis in Pregnancy: Multi-Disciplinary Guidelines From an Academic Medical Center. *Front. Surg.* **2021**, *8*, 796876. [CrossRef]
11. Sakamoto, J.; Michels, C.; Eisfelder, B.; Joshi, N. Trauma in Pregnancy. *Emerg. Med. Clin. N. Am.* **2019**, *37*, 317–338. [CrossRef] [PubMed]
12. The American College of Obstetricians and Gynecologists. Committee Opinion No. 723: Guidelines for Diagnostic Imaging During Pregnancy and Lactation. *Obstet. Gynecol.* **2017**, *130*, e210–e216. [CrossRef]
13. Flanagan, E.; Bell, S. Abdominal Imaging in Pregnancy (Maternal and Foetal Risks). *Best. Pract. Res. Clin. Gastroenterol.* **2020**, *44–45*, 101664. [CrossRef]
14. International Commission on Radiological Protection. Pregnancy and medical radiation. *Ann. ICRP* **2000**, *30*, 1–43. [PubMed]
15. European Commission. *Radiation Protection RP100: Guidance for Protection of Unborn Children and Infants Irradiated due to Parental Medical Exposures*; Publications Office: Luxembourg, 1999.
16. Valentin, J. Editorial. *Ann. ICRP* **2000**, *30*, iii–iv. [CrossRef]
17. Tremblay, E.; Thérasse, E.; Thomassin-Naggara, I.; Trop, I. Quality Initiatives: Guidelines for Use of Medical Imaging during Pregnancy and Lactation. *RadioGraphics* **2012**, *32*, 897–911. [CrossRef]
18. Matsunaga, Y.; Haba, T.; Kobayashi, M.; Suzuki, S.; Asada, Y.; Chida, K. Fetal Radiation Dose of Four Tube Voltages in Abdominal CT Examinations during Pregnancy: A Phantom Study. *J. Appl. Clin. Med. Phys.* **2021**, *22*, 178–184. [CrossRef]
19. Hurwitz, L.M.; Yoshizumi, T.; Reiman, R.E.; Goodman, P.C.; Paulson, E.K.; Frush, D.P.; Toncheva, G.; Nguyen, G.; Barnes, L. Radiation Dose to the Fetus from Body MDCT During Early Gestation. *Am. J. Roentgenol.* **2006**, *186*, 871–876. [CrossRef]
20. Faj, D.; Bassinet, C.; Brkić, H.; De Monte, F.; Dreuil, S.; Dupont, L.; Ferrari, P.; Gallagher, A.; Gallo, L.; Huet, C.; et al. Management of Pregnant or Potentially Pregnant Patients Undergoing Diagnostic and Interventional Radiology Procedures: Investigation of Clinical Routine Practice. *Phys. Medica* **2023**, *115*, 103159. [CrossRef] [PubMed]
21. Gilet, A.G.; Dunkin, J.M.; Fernandez, T.J.; Button, T.M.; Budorick, N.E. Fetal Radiation Dose During Gestation Estimated on an Anthropomorphic Phantom for Three Generations of CT Scanners. *Am. J. Roentgenol.* **2011**, *196*, 1133–1137. [CrossRef]
22. Osei, E.K.; Darko, J. Foetal radiation dose and risk from diagnostic radiology procedures: A multinational study. *ISRN Radiol.* **2012**, *2013*, 318425. [CrossRef] [PubMed] [PubMed Central]
23. Kopacin, V.; Kasabasic, M.; Faj, D.; de Saint Hubert, M.; Galic, S.; Ivkovic, A.; Majer, M.; Brkic, H. Development of a Computational Pregnant Female Phantom and Calculation of Fetal Dose during a Photon Breast Radiotherapy. *Radiol. Oncol.* **2022**, *56*, 541–551. [CrossRef]
24. Kopačin, V.; Brkić, H.; Ivković, A.; Kasabašić, M.; Knežević, Ž.; Majer, M.; Nodilo, M.; Turk, T.; Faj, D. Development and Validation of the Low-Cost Pregnant Female Physical Phantom for Fetal Dosimetry in MV Photon Radiotherapy. *J. Appl. Clin. Med. Phys.* **2024**, *25*, e14240. [CrossRef] [PubMed]
25. Knežević, Ž.; Beck, N.; Milković, Đ.; Miljanić, S.; Ranogajec-Komor, M. Characterisation of RPL and TL Dosimetry Systems and Comparison in Medical Dosimetry Applications. *Radiat. Meas.* **2011**, *46*, 1582–1585. [CrossRef]
26. ATGC. *Explanation Material of RPL Glass Dosimeter: Small Element System*; Asahi Techno Glass Corporation: Tokyo, Japan, 2007.
27. Vekić, B.; Ban, R.; Miljanić, S. Secondary Standard Dosimetry Laboratory at the Ruđer Bošković Institute. *Arh. Hig. Rada Toksikol.* **2006**, *57*, 189–194. [PubMed]
28. Knežević, Ž.; Stolarczyk, L.; Bessieres, I.; Bordy, J.M.; Miljanić, S.; Olko, P. Photon Dosimetry Methods Outside the Target Volume in Radiation Therapy: Optically Stimulated Luminescence (OSL), Thermoluminescence (TL) and Radiophotoluminescence (RPL) Dosimetry. *Radiat. Meas.* **2013**, *57*, 9–18. [CrossRef]
29. ACR-SPR Practice Parameter for Imaging Pregnant or Potentially Pregnant Adolescents and Patients with Ionizing Radiation [Revised 2023 (Resolution 31)]. Available online: <https://www.acr.org/-/media/ACR/Files/Practice-Parameters/Pregnant-Pts.pdf> (accessed on 17 November 2024).
30. Niemann, T.; Nicolas, G.; Roser, H.W.; Müller-Brand, J.; Bongartz, G. Imaging for Suspected Pulmonary Embolism in Pregnancy—What about the Fetal Dose? A Comprehensive Review of the Literature. *Insights Imaging* **2010**, *1*, 361–372. [CrossRef]
31. Gillespie, C.D.; Yates, A.; Hughes, M.; Ewins, K.; McMahon, G.; Hynes, J.; Murphy, M.C.; Galligan, M.; Vencken, S.; Alih, E.; et al. Validating the Safety of Low-Dose CTPA in Pregnancy: Results from the OPTICA (Optimised CT Pulmonary Angiography in Pregnancy) Study. *Eur. Radiol.* **2024**, *34*, 4864–4873. [CrossRef]
32. Tse, G.H.; Balian, V.; Charalampatou, P.; Maliakal, P.; Nayak, S.; Dyde, R.; Nagaraja, S. Foetal Radiation Exposure Caused by Mechanical Thrombectomy in Large-Vessel Ischaemic Stroke in Pregnancy. *Neuroradiology* **2019**, *61*, 443–449. [CrossRef] [PubMed]
33. James, B.; Kelly, B. The Abdominal Radiograph. *Ulster Med. J.* **2013**, *82*, 179–187.
34. Fachgesellschaften, Arbeitsgemeinschaft der Wissenschaftlichen Medizinischen. “S3-Leitlinie Polytrauma”. Available online: https://register.awmf.org/assets/guidelines/012_D_Ges_fuer_Unfallchirurgie/012-019m_S3_Polytrauma_Schwererletzten-Behandlung_2016-09-abgelaufen.pdf (accessed on 15 November 2024).

35. Kahn, J.; Kaul, D.; Böning, G.; Rotzinger, R.; Freyhardt, P.; Schwabe, P.; Maurer, M.; Renz, D.; Streitparth, F. Quality and Dose Optimized CT Trauma Protocol—Recommendation from a University Level-I Trauma Center. *RöFo* **2017**, *189*, 844–854. [[CrossRef](#)] [[PubMed](#)]
36. Yaniv, G.; Portnoy, O.; Simon, D.; Bader, S.; Konen, E.; Guranda, L. Revised Protocol for Whole-Body CT for Multi-Trauma Patients Applying Triphasic Injection Followed by a Single-Pass Scan on a 64-MDCT. *Clin. Radiol.* **2013**, *68*, 668–675. [[CrossRef](#)] [[PubMed](#)]
37. Naulet, P.; Wassel, J.; Gervaise, A.; Blum, A. Evaluation of the Value of Abdominopelvic Acquisition without Contrast Injection When Performing a Whole Body CT Scan in a Patient Who May Have Multiple Trauma. *Diagn. Interv. Imaging* **2013**, *94*, 410–417. [[CrossRef](#)] [[PubMed](#)]
38. The Royal College of Radiologists. *Standards of Practice and Guidance for Trauma Radiology in Severely Injured Patients*, 2nd ed.; The Royal College of Radiologists: London, UK, 2015.

Disclaimer/Publisher’s Note: The statements, opinions and data contained in all publications are solely those of the individual author(s) and contributor(s) and not of MDPI and/or the editor(s). MDPI and/or the editor(s) disclaim responsibility for any injury to people or property resulting from any ideas, methods, instructions or products referred to in the content.